J. Fluid Mech. (1981), *vol.* 110, *pp.* 255–272
Printed in Great Britain

The stress tensor in a granular flow at high shear rates

By S. B. SAVAGE
Department of Civil Engineering and Applied Mechanics,
McGill University, Canada
AND D. J. JEFFREY
Department of Applied Mathematics and Theoretical Physics,
Silver Street, Cambridge

(Received 8 July 1980)

The stress tensor in a granular shear flow is calculated by supposing that binary collisions between the particles comprising the granular mass are responsible for most of the momentum transport. We assume that the particles are smooth, hard, elastic spheres and express the stress as an integral containing probability distribution functions for the velocities of the particles and for their spatial arrangement. By assuming that the single-particle velocity distribution function is Maxwellian and that the spatial pair distribution function is given by a formula due to Carnahan & Starling, we reduce this integral to one depending upon a single non-dimensional parameter R: the ratio of the characteristic mean shear velocity to the root mean square of the precollisional particle-velocity perturbation. The integral is evaluated asymptotically for $R \gg 1$ and $R \ll 1$ and numerically for intermediate values. Good agreement is found between the stresses measured in experiments on dry granular materials and the theoretical predictions when R is given the value 1·7. This case is probably the one for which the present analysis is most appropriate. For moderate and large values of R, the theory predicts both shear and normal stresses that are proportional to the square of the particle diameter and the square of the shear rate, and depend strongly on the solids volume fraction. A provisional comparison is made between the stresses predicted in the limit $R \to \infty$ and the experimental results of Bagnold for shear flow of neutrally buoyant wax spheres suspended in water. The predicted stresses are of the correct order of magnitude and yield the proper variation of stress with concentration. When $R \ll 1$, the shear stress is linear in the shear rate, and the analysis can be applied to shear flow in a fluidized bed, although such an application is not developed further here.

1. Introduction

There have been few investigations of the rheological properties of dense concentrations of large particles immersed in fluids for cases in which inertia effects are dominant. The relative rarity of these investigations is probably due more to the difficulties there are in performing experiments and the lack of any obvious theoretical approach than to any lack of importance. In fact, an understanding of such flows could be of great benefit in connection with numerous practical applications involving, for example, slurry pipelines, sediment transport, pneumatic transport, materials handling equipment, and fluidized beds. Of the work that has been done on the rheology of

concentrated suspensions of particles (for example, see reviews by Goldsmith & Mason 1967; Batchelor 1976; Jeffrey & Acrivos 1976; Gadala-Maria 1979) most have dealt with small particles at low Reynolds numbers. With reference to larger particles, Cheng & Richmond (1978) have discussed some of the phenomena that can arise in flows of dense solid–liquid mixtures, such as yield stresses, slip–stick behaviour, normal stress effects, discontinuous changes in stresses, wall effects, and liquefaction. Because of the similarities to the behaviour of dry particulate materials, they have termed these flows 'granulo-viscous'.

The most extensive and consistent experiments on the rheology of granular flows yet performed appear to be those of Bagnold (1954). Neutrally buoyant spherical particles suspended in Newtonian fluids (water and a glycerine–water–alcohol mixture) were sheared in the annular region between a stationary inner cylinder and a concentric rotating outer cylinder. Both the torque and the normal stress in the radial direction were measured as functions of the shear rate for various values of mean solids concentration. Bagnold distinguished two limiting types of behaviour. In the so-called *macro-viscous* region (corresponding to low shear rates), which is dominated by fluid viscosity, the shear and the normal stress are linearly proportional to the shear rate. Bagnold attributed the presence of the normal stress in the radial direction to an anisotropy in the spatial particle distribution. In the *grain-inertia* region, which is the main concern of the present paper, the fluid in the interstices plays a minor role and the dominant effects arise from particle–particle interactions. Bagnold argued that the main mechanism for momentum transfer is the succession of glancing collisions as the grains of one layer overtake those of the adjacent slower layer. Both the change in momentum during a single collision and the rate at which collisions occur are proportional to the relative velocity of the two layers. Thus, both the shear and normal stresses in this region vary as the square of the shear rate. Bagnold's experiments at higher shear rates clearly showed this kind of dependence. Bagnold also found that the stresses increased strongly with solids concentration, particularly at the higher concentrations approaching the maximum possible solids volume fraction.

While there have been some proposals for constitutive equations which are based wholly or in part upon a continuum mechanics approach and make use of Bagnold's experimental data (Jenkins & Cowin 1979; Kanatani 1979; McTigue 1979; Savage 1979), only McTigue (1978) has attempted to analyse the collisional dynamics of the microstructure and improve upon Bagnold's simple flow model of the *grain inertia* region. His approach follows Marble's (1964) suggestive analysis of particle collisions in a one-dimensional flow of a gas containing solid particles of two different sizes and Soo's (1967) closely related analysis of stresses due to collisions in a particle cloud subjected to shear. McTigue's model is highly simplified in that he ignores particle fluctuations, constrains the particles to translate with the mean motion and neglects higher-order effects of concentration upon collision frequency. Although he shows that the stresses depend upon the square of the shear rate, the predicted stresses are between one and two orders of magnitude lower than Bagnold's measurements and the dependence of the stress upon the solids concentration is poorly represented.

In the present paper we examine the bulk stresses developed when a dispersion of hard elastic spherical particles is subjected to a bulk deforming motion. The effects of the interstitial fluid upon the generation of the bulk stresses will be neglected. This

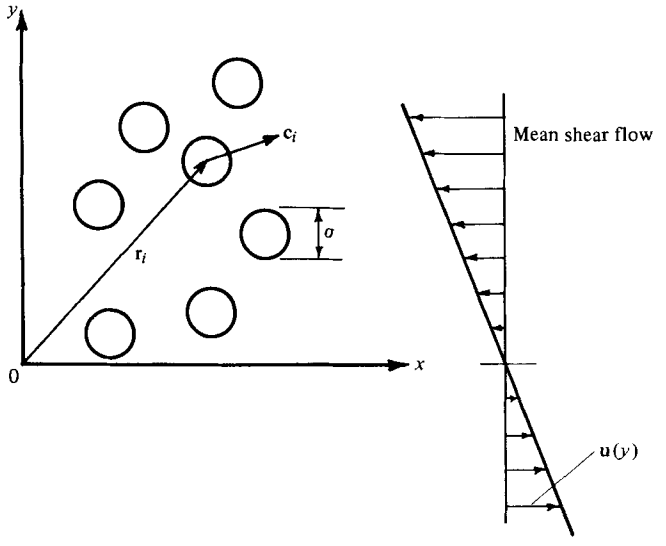

FIGURE 1. Granular shear flow.

seems physically plausible if the interstitial fluid is a gas but less obvious if, for example, the fluid is a liquid of the same density as the solid particles. Bagnold (1954) reasoned that, in flow regimes where grain inertia is dominant, the motion of the liquid displaced by the particle fluctuations is random and thus is unlikely to give rise to any net contribution to the stresses. However, his argument is not overly convincing to us. Thus, we caution against the indiscriminate application of the present analysis to cases in which the particle and fluid densities are similar.

There remain three primary mechanisms by which the bulk stresses can be generated; they are (i) dry friction, (ii) transport of momentum by particle translation, and (iii) momentum transport by particle interactions. Although all three can co-exist in certain flow regimes, usually one of them will play a predominant role. At high solids concentration and low shear rates, the particles are in close rubbing contact, grain inertia effects are small and the stresses are of the *quasi-static*, rate-independent, Coulomb type described in the soil mechanics literature (Schofield & Wroth 1968) dealing with dry cohesionless granular materials like sand. At very low concentrations and high shear rates, we might expect the granular material to behave like a dilute gas. The mean free path is large compared with the particle diameter, and the shear stress, for example, results from the interchange of particles between adjacent layers of 'fluid' moving at different velocities. When both the concentration and the shear rate are moderately high, the situation is analogous to a simple liquid where the exchange of momentum occurs primarily by the continuous action of intermolecular forces (Temperley, Rowlinson & Rushbrooke 1968; Faber 1972; Hansen & McDonald 1976). The granular flow mechanics bear similarities to the 'hard-sphere models' used in the statistical-mechanical theories of the liquid state where the intermolecular forces are impulsive forces associated with particle collisions.

The latter flow regime is the main concern of this paper. Since the solids concentration is not low, only rarely will there form vacancies of sufficient size to permit particle transport between adjacent shear layers. On the other hand, we consider high enough

shear rates and moderately high concentrations so that the majority of particle interactions are collisions over very short time intervals and dry frictional rubbing contacts are relatively infrequent.

2. General integral form for the stress tensor

We consider a dispersion of identical, hard, elastic, spherical particles of diameter σ subjected to a mean shearing motion $\mathbf{u} = u(y)\,\mathbf{e}_x$ where $\mathbf{e}_x$ is the unit vector in the x-direction (figure 1). Because of interparticle collisions, the instantaneous particle velocity $\mathbf{c}_i(\mathbf{r}_i, t)$ differs from the mean translational velocity $\mathbf{u}(y)$ by a random fluctuating component. Since we are considering hard spheres such that the collisions are almost instantaneous, the probability of many-body collisions is assumed negligible, so we need treat only binary collisions. The assumption no doubt seriously breaks down at very high concentrations, say solid fractions $\nu \gtrsim 0{\cdot}5$, when it becomes likely that groups of particles intermittently, at least, lock together and prolonged sliding contacts occur. In order to calculate the collisional transport of momentum and hence determine the stress tensor, we require a description of the precollisional correlation of particle positions and velocities. Let us first consider the spatial particle distributions.

2.1. *Configurational and collisional distribution functions*

We shall define an *L-particle configurational distribution function* $n^{(L)}(\mathbf{r}_1, \mathbf{r}_2, \ldots, \mathbf{r}_L))$ such that $n^{(L)}(\mathbf{r}_1, \mathbf{r}_2, \ldots, \mathbf{r}_L)\,\delta\mathbf{r}_1 \ldots \delta\mathbf{r}_L$ is the probability of finding a particle in each of the volume elements $\delta\mathbf{r}_1, \delta\mathbf{r}_2, \ldots, \delta\mathbf{r}_L$ centred on $\mathbf{r}_1, \mathbf{r}_2, \ldots, \mathbf{r}_L$ (where $L = 1, 2, 3, \ldots$). The *one-particle distribution function* $n^{(1)}(\mathbf{r})$ is just the number density n of particles at $\mathbf{r}$. For a homogeneous bulk it has a uniform value

$$n^{(1)}(\mathbf{r}) = N/V = n, \tag{2.1}$$

where N is the mean number of particles in the volume V.

In an amorphous mass of particles there is only a short-range order and there is no correlation between particles that are far apart. Thus the joint probability of finding particles at $\mathbf{r}_1$ and $\mathbf{r}_2$ when $\mathbf{r}_1$ and $\mathbf{r}_2$ are far apart is the product of the individual probabilities, that is,

$$n^{(2)}(\mathbf{r}_1, \mathbf{r}_2) \sim n^{(1)}(\mathbf{r}_1)\, n^{(1)}(\mathbf{r}_2) = n^2 \quad \text{for} \quad |\mathbf{r}_2 - \mathbf{r}_1| \gg \sigma. \tag{2.2}$$

It is convenient to define a *configurational pair-correlation function*

$$g(\mathbf{r}_1, \mathbf{r}_2) = n^{(2)}(\mathbf{r}_1, \mathbf{r}_2)/n^2, \tag{2.3}$$

so that

$$g(\mathbf{r}_1, \mathbf{r}_2) \to 1 \quad \text{as} \quad |\mathbf{r}_2 - \mathbf{r}_1| \to \infty.$$

In structural studies of the liquid state, $g(\mathbf{r}_1, \mathbf{r}_2)$ is of great importance for the determination of the thermodynamic properties; an extensive literature concerned both with its experimental measurement and its theoretical prediction now exists (see reviews in Temperley *et al.* 1968; Henderson 1971; Reed & Gubbins 1973; Croxton 1974; Hansen & McDonald 1976; Ziman 1979). In dense fluids at equilibrium (no mean deformation) there is spatial homogeneity and $g(\mathbf{r}_1, \mathbf{r}_2)$ depends only upon the separation distance $r = |\mathbf{r}_2 - \mathbf{r}_1|$. Then $g = g_0(r)$ is termed the *radial distribution function*; it can be interpreted as the ratio of the local number density at a distance r from the central particle to the bulk number density. The simplest intermolecular potential

energy function that can be used to determine the thermodynamic properties is the hard-sphere model. The radial distribution function for this structural model has been theoretically determined both by analytical approaches (Thiele 1963; Wertheim 1963; Lebowitz 1964; Baxter 1968, 1971) as well as by numerical methods (Alder & Hoover 1968; Wood 1968; Baxter 1971; Ree 1971) involving Monte Carlo methods and molecular dynamic calculations.

Carnahan & Starling (1969) proposed a semi-empirical equation of state from which they obtained the radial distribution function at contact ($r = \sigma$) for single-component, and mixtures (Mansoori *et al.* 1971) of, hard-sphere fluids. For a system of identical spheres, it can be written in terms of the solids fraction ν as

$$g_0(\sigma;\nu) = \frac{1}{(1-\nu)} + \frac{3\nu}{2(1-\nu)^2} + \frac{\nu^2}{2(1-\nu)^3}. \tag{2.4}$$

Their expression is in almost exact agreement with the 'exact' numerical molecular dynamics calculations for values of ν up to about 0·5. But above this it gives values of $g_0(\sigma;\nu)$ that are too low.

If the bulk of particles is subjected to a mean shear flow, the radial distribution function, which is spherical in equilibrium, becomes distorted into an ellipsoidal distribution whose principal axes are determined by the mean deformation field. For the usual dense gases or liquids, the mean shear is small and causes only a small perturbation to the equilibrium radial distribution function. Born & Green (1947), Kirkwood, Buff & Green (1949) and Green (1969) have discussed such perturbations but their analyses are of limited interest to the present granular-flow problems. Green gave the form of the perturbation but not quantitative values, whereas the analysis of Kirkwood, Buff & Green involved the Brownian motion friction coefficient for which there is no counterpart in the granular-flow situation. Moreover, for the present problems, the mean shear is not always small. Let us define a velocity scale associated with the mean shear, say $\sigma du/dy$. While this is very small compared with the root-mean-square fluctuation velocity in the context of the molecular description of dense fluids, in the case of granular flows the two velocities can be of the same order.

In the present analysis we shall determine the anisotropy in the *collisional pair distribution function* by making use of a kinematic argument. It should be noted that the overall theory will be applied to the analysis of two somewhat different kinds of flows: a pure granular shear flow and the shear flow of a fluidized bed. In the granular shear flow the magnitude of the particle velocity fluctuations is linked directly to the strength of the shear flow, whereas in the fluidized bed the particle velocity fluctuations are affected by the mean shear, but are generated primarily by the fluidizing fluid (for the case of small shear).

Let us assume that the single particle velocity distribution function $f^{(1)}(\mathbf{c}, \mathbf{r})$ (defined such that $f^{(1)}(\mathbf{c}, \mathbf{r})\,\delta\mathbf{c}$ is the differential number of particles per unit volume with velocities within the range $\mathbf{c}$ and $\mathbf{c} + \delta\mathbf{c}$) is Maxwellian about the local mean transport velocity. The experiments of Carlos & Richardson (1968) show that there is some justification for this assumption, at least for the case of fluidized beds. If we consider a sphere moving instantaneously with the mean transport velocity, then, because of the mean shear, this sphere is more likely to experience collisions from other particles on its surface corresponding to the two 'upstream' quadrants (figure 2). We shall now put this intuitive notion into more quantitative terms.

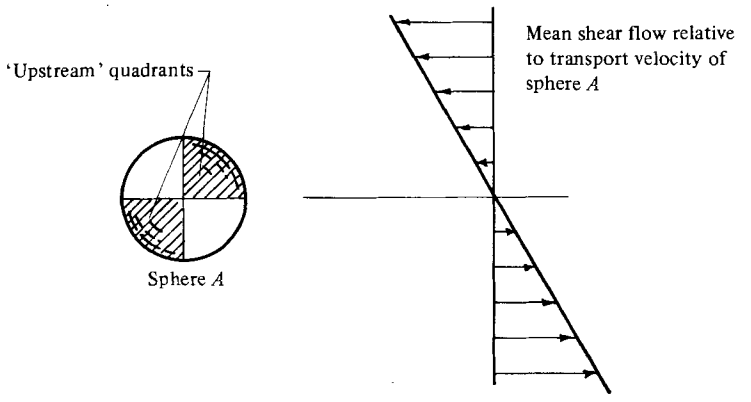

FIGURE 2. Anisotropy in collisional pair distribution function arising from mean shear. Sphere A is instantaneously moving with the mean transport velocity, and the shaded 'upstream' quadrants receive more collisions than the downstream ones.

A complete pair distribution function $f^{(2)}(\mathbf{c}_1, \mathbf{r}_1, \mathbf{c}_2, \mathbf{r}_2, t)$ is defined such that

$$f^{(2)}(\mathbf{c}_1, \mathbf{r}_1, \mathbf{c}_2, \mathbf{r}_2, t)\, \delta\mathbf{c}_1 \delta\mathbf{c}_2 \delta\mathbf{r}_1 \delta\mathbf{r}_2 \tag{2.5}$$

is the probability of finding a pair of particles in the volume elements $\delta\mathbf{r}_1, \delta\mathbf{r}_2$ centred on the points $\mathbf{r}_1, \mathbf{r}_2$ and having velocities within the ranges $\mathbf{c}_1$ and $\mathbf{c}_1 + \delta\mathbf{c}_1$, and $\mathbf{c}_2$ and $\mathbf{c}_2 + \delta\mathbf{c}_2$. We now assume that the complete pair distribution function can be expressed as the product of the spatial pair distribution function and the two single particle velocity distribution functions, thus

$$f^{(2)}(\mathbf{c}_1, \mathbf{r}_1, \mathbf{c}_2, \mathbf{r}_2, t) = \frac{n^{(2)}(\mathbf{r}_1, \mathbf{r}_2, t)}{n^2} f^{(1)}(\mathbf{c}_1, \mathbf{r}_1, t) f^{(1)}(\mathbf{c}_2, \mathbf{r}_2, t), \tag{2.6}$$

where

$$n^{(2)}/n^2 = g(\mathbf{r}_1, \mathbf{r}_2, t). \tag{2.7}$$

If we integrate $f^{(2)}$ over all possible values of the velocities for particles 1 and 2, then

$$\int f^{(2)} d\mathbf{c}_1 d\mathbf{c}_2 = n^{(2)}. \tag{2.8}$$

Consider two spheres in contact at $\mathbf{r}$ as shown in figure 3 such that $\mathbf{r}_1 = \mathbf{r} - \frac{1}{2}\sigma\mathbf{k}$ and $\mathbf{r}_2 = \mathbf{r} + \frac{1}{2}\sigma\mathbf{k}$, where $\mathbf{k}$ is the unit vector along the line of centres at collision and the spheres' relative velocity $\mathbf{q} = \mathbf{c}_1 - \mathbf{c}_2$. In the *equilibrium* situation ($f^{(2)} = f_0^{(2)}$) at contact, equation (2.8) can be written as

$$\int f_0^{(2)}(\mathbf{c}_1, \mathbf{c}_2, \sigma)\, d\mathbf{c}_1 d\mathbf{c}_2 = n_0^{(2)}(\sigma) = n^2 g_0(\sigma; \nu) = 2 \int_{\mathbf{q}.\mathbf{k}>0} f_0^{(2)} d\mathbf{c}_1 d\mathbf{c}_2. \tag{2.9}$$

While the first integral of (2.9) is taken over all possible values of $\mathbf{c}_1$ and $\mathbf{c}_2$, the last integral is taken only over values of $\mathbf{c}_1$ and $\mathbf{c}_2$ such that $\mathbf{q} \cdot \mathbf{k} > 0$ (this latter condition picks out particles that are just about to collide; $\mathbf{q} \cdot \mathbf{k} < 0$ corresponds to those that have just collided). For the *non-equilibrium* case (with steady mean shear flow $\mathbf{u}(y)$) at contact, we take

$$\int f^{(2)} d\mathbf{c}_1 d\mathbf{c}_2 = n^2 g(\mathbf{r}_1, \mathbf{r}_2) = 2 \int_{\mathbf{q}.\mathbf{k}>0} g_0(\sigma; \nu) f^{(1)}(\mathbf{c}_1, \mathbf{r}_1; \mathbf{u}(\mathbf{r}_1)) f^{(1)}(\mathbf{c}_2, \mathbf{r}_2; \mathbf{u}(\mathbf{r}_2))\, d\mathbf{c}_1 d\mathbf{c}_2. \tag{2.10}$$

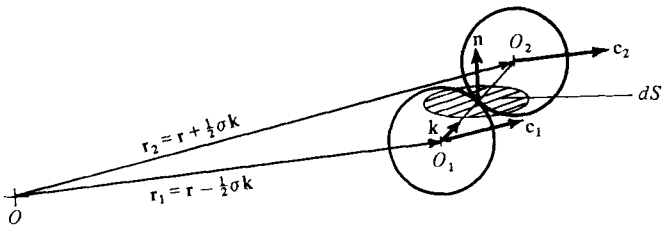

FIGURE 3. Geometry of a collision of two spheres.

We have assumed in (2.10) that the *spatial pair distribution function* is the same as the spherically symmetric equilibrium radial distribution function $g_0(\sigma;\nu)$ at contact. However, because of the presence of the mean shear $\mathbf{u}$, the *collisional pair distribution function* $g(\mathbf{r}_1, \mathbf{r}_2)$ is different from $g_0(\sigma;\nu)$. In other words, if we were to take a snapshot of the flow, the *distribution of particles* might appear to be isotropic but the *distribution of collisions* could be anisotropic in the case in which there was a mean shear.

Thus from (2.10)

$$g(\mathbf{r}_1, \mathbf{r}_2) = \frac{2g_0(\sigma;\nu)}{n^2} \int_{\mathbf{q}.\mathbf{k}>0} f^{(1)}(\mathbf{c}_1, \mathbf{r}_1; \mathbf{u}(\mathbf{r}_1)) f^{(1)}(\mathbf{c}_2, \mathbf{r}_2; \mathbf{u}(\mathbf{r}_2))\, d\mathbf{c}_1 d\mathbf{c}_2, \tag{2.11}$$

and by making use of Carnahan & Starling's expression (2.4) for the radial distribution function $g_0(\sigma;\nu)$, $g(\mathbf{r}_1, \mathbf{r}_2)$ may then be explicitly determined.

Assuming the single particle velocity distribution functions are Maxwellian,† for example,

$$f^{(1)}(\mathbf{c}_1, \mathbf{r}_1; \mathbf{u}(\mathbf{r}_1)) = n(\pi\overline{v^2})^{-\frac{3}{2}} \exp\{-(\mathbf{c}_1 - \mathbf{u}(\mathbf{r}_1))^2/\overline{v^2}\}, \tag{2.12}$$

where $\overline{V^2}$ is the mean square of the precollision particle velocity perturbation. After substituting expressions for the velocity distribution functions like (2.12) into (2.11) and transforming the variables from $\mathbf{c}_1$, $\mathbf{c}_2$ to $\mathbf{Q}$, $\mathbf{q}$, where $\mathbf{Q}$ is the velocity of the centre of mass of the two particles and $\mathbf{q}$ is the relative velocity $\mathbf{c}_1 - \mathbf{c}_2$, (2.11) may be integrated to yield

$$g(\mathbf{r}_1, \mathbf{r}_2) = g_0(\sigma;\nu) \operatorname{erfc}(2\mathbf{k}\,.\,\mathbf{u}(\mathbf{r}_2)/(2\overline{v^2})^{\frac{1}{2}}), \tag{2.13}$$

where $\operatorname{erfc}(x)$ is the complementary error function

$$\operatorname{erfc}(x) = \frac{2}{\pi^{\frac{1}{2}}} \int_x^\infty e^{-x^2} dx. \tag{2.14}$$

The product of $\mathbf{k}\,.\,\mathbf{u}(\mathbf{r}_2)$ may be expressed in terms of the spherical co-ordinates θ and ϕ (figure 4) as

$$\mathbf{k}\,.\,\mathbf{u}(\mathbf{r}_2) = -\tfrac{1}{2}\sigma|du/dy| \cos\phi \cos\theta \sin\theta. \tag{2.15}$$

Figure 5 shows the variation of $g(\mathbf{r}_1, \mathbf{r}_2)/g_0(\sigma;\nu)$ with θ for various values of $2^{-\frac{1}{2}}R\cos\phi$, where

$$R = \sigma|du/dy|/\overline{v^2}^{\frac{1}{2}} \tag{2.16}$$

is the ratio of mean shear characteristic velocity to the r.m.s. precollision velocity

† In reality the velocity fluctuations are likely to be anisotropic and the distribution function may depart from the exponential form. Nevertheless, departures from a Maxwellian distribution are expected to produce only minor changes in the numerical coefficients associated with the components of the stress tensor, leaving the functional form of the final expressions for these components unchanged.

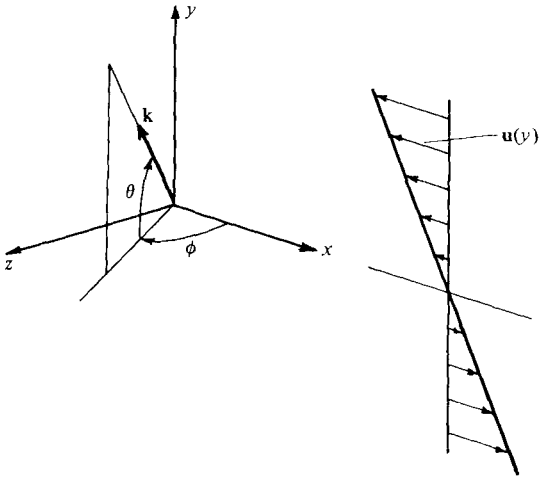

FIGURE 4. Definition of co-ordinate system.

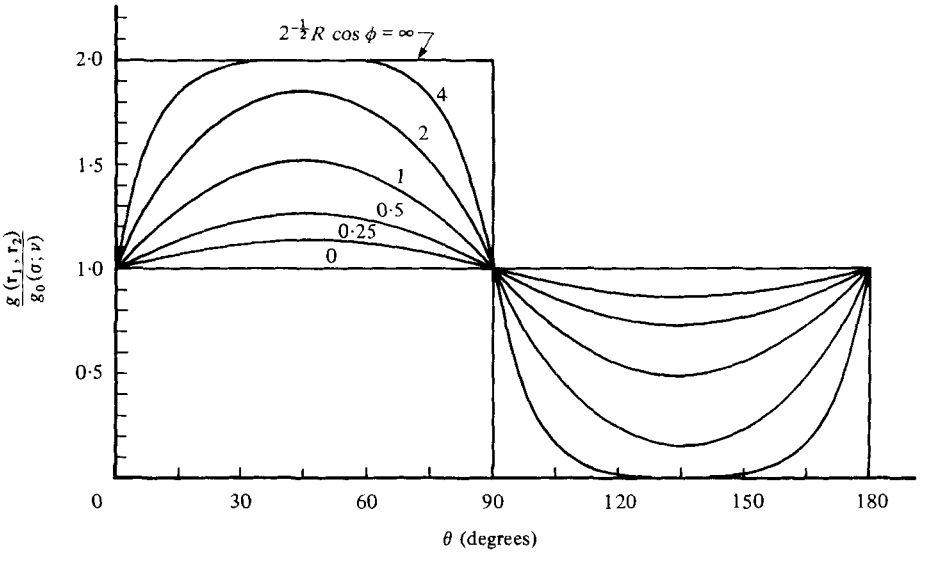

FIGURE 5. Collisional pair distribution function.

perturbation. For small values of R, $g(\mathbf{r}_1, \mathbf{r}_2)$ is ellipsoidal, whereas for large R the variations in $g(\mathbf{r}_1, \mathbf{r}_2)$ are step-like.

2.2. *Collisional transfer of momentum*

To obtain the integral expression for the stress tensor, we follow a treatment similar to Enskog's analysis of the collisional transfer of molecular properties in a dense gas, as described by Chapman & Cowling (1970). Consider two particles colliding at the point $\mathbf{r}$ as shown in figure 3; $\sigma^2 \delta\mathbf{k}$ is the surface element on a sphere of radius σ and centre O_2 on which O_1 must lie at collision. In time δt prior to the collision, O_1 moved through a distance $q\,\delta t$ relative to O_2. For a collision to occur within δt then, O_1 must lie inside the volume $\sigma^2 \delta\mathbf{k}(\mathbf{q} \cdot \mathbf{k})\,\delta t$. To determine the stress tensor, we must consider

the collisional transfer of momentum across the area element δS whose unit normal is $\mathbf{n}$ (figure 3). If the line of centres at collision, which is of length σ, is to cut δS, then O_2 must lie within the volume $\sigma(\mathbf{k}\,.\,\mathbf{n})\,\delta S$, where $\mathbf{k}\,.\,\mathbf{n}$ is drawn as positive in figure 3. Thus, the probable number of collisions per unit time in which $\mathbf{c}_1$, $\mathbf{c}_2$ and $\mathbf{k}$ lie within the ranges $\delta\mathbf{c}_1, \delta\mathbf{c}_2, \delta\mathbf{k}$ is

$$g(\mathbf{r}_1, \mathbf{r}_2) f^{(1)}(\mathbf{c}_1, \mathbf{r}_1; \mathbf{u}(\mathbf{r}_1)) f^{(1)}(\mathbf{c}_2, \mathbf{r}_2; \mathbf{u}(\mathbf{r}_2))\, \sigma^2 \delta\mathbf{k}(\mathbf{q}\,.\,\mathbf{k})\, \sigma(\mathbf{k}\,.\,\mathbf{n}) \delta S\, \delta\mathbf{c}_1 \delta\mathbf{c}_2. \tag{2.17}$$

Each collision causes a particle on the positive side of δS to gain momentum $m(\mathbf{c}_2' - \mathbf{c}_2)$ at the expense of one on the negative side (where $\mathbf{c}_2'$ is the velocity of particle 2 after the collision). The total rate of transfer of momentum across δS per unit time and area for this type of collision is thus

$$m\sigma^3 \int (\mathbf{c}_2' - \mathbf{c}_2)\, g(\mathbf{r}_1, \mathbf{r}_2) f^{(1)}(\mathbf{c}_1, \mathbf{r}_1; \mathbf{u}(\mathbf{r}_1)) f^{(1)}(\mathbf{c}_2, \mathbf{r}_2; \mathbf{u}(\mathbf{r}_2))\, (\mathbf{q}\,.\,\mathbf{k})\, (\mathbf{k}\,.\,\mathbf{n})\, d\mathbf{k}\, d\mathbf{c}_1 d\mathbf{c}_2, \tag{2.18}$$

integrated over all values such that $\mathbf{q}\,.\,\mathbf{k} > 0$ and $\mathbf{k}\,.\,\mathbf{n} > 0$. If we interchange the role of the colliding particles, i.e. $\mathbf{k} \to -\mathbf{k}, \mathbf{q} \to -\mathbf{q}$, $(\mathbf{c}_2' - \mathbf{c}_2) \to (\mathbf{c}_1' - \mathbf{c}_1) = -(\mathbf{c}_2' - \mathbf{c}_2)$, then we obtain the same integral as (2.18) but now integrated over all values such that $\mathbf{q}\,.\,\mathbf{k} > 0$ and $\mathbf{k}\,.\,\mathbf{n} < 0$. Thus, the total rate of momentum transfer per unit time and area may be written as $\frac{1}{2}$ of the integral expressed by (2.17), but integrated over all values such that $\mathbf{q}\,.\,\mathbf{k} > 0$. This expression is the scalar product of $\mathbf{n}$ and another vector which represents the vector momentum flux. If we consider the dynamics of a collision, it can be shown (Chapman & Cowling 1970) that $\mathbf{c}_2' - \mathbf{c}_2 = (\mathbf{q}\,.\,\mathbf{k})\,\mathbf{k}$. The stress tensor arising from interparticle collisions may thus be written as

$$\mathbf{T} = -\frac{m}{2}\sigma^3 \int_{\mathbf{q}.\mathbf{k}>0} g(\mathbf{r}_1, \mathbf{r}_2) f^{(1)}(\mathbf{c}_1, \mathbf{r}_1; \mathbf{u}(\mathbf{r}_1)) f^{(1)}(\mathbf{c}_2, \mathbf{r}_2; \mathbf{u}(\mathbf{r}_2))\, (\mathbf{q}\,.\,\mathbf{k})^2\, \mathbf{kk}\, d\mathbf{k}\, d\mathbf{c}_1 d\mathbf{c}_2, \tag{2.19}$$

where $\mathbf{kk}$ is a dyadic product and the integral is taken over all values such that $\mathbf{q}\,.\,\mathbf{k} > 0$. Again assuming the single-particle velocity distribution function to be Maxwellian as in (2.12) and transferring to the variables $\mathbf{Q}$, the centre of mass velocity, and $\mathbf{q}$, several of the integrations in (2.19) can be performed to yield

$$\mathbf{T} = -\tfrac{1}{2} m\sigma^3 n^2 (2\pi\overline{v^2})^{-\frac{1}{2}} \times \int_{\mathbf{q}.\mathbf{k}>0} \mathbf{kk}\, g(\mathbf{r}_1, \mathbf{r}_2)\, (\mathbf{q}\,.\,\mathbf{k})^2 \exp\left\{\frac{-1}{2\overline{v^2}}\, (\mathbf{q}\,.\,\mathbf{k} + 2\mathbf{k}\,.\,\mathbf{u}(\mathbf{r}_2))^2\right\} d\mathbf{k}\, d(\mathbf{q}\,.\,\mathbf{k}). \tag{2.20}$$

From figure 4 it may be seen that

$$\mathbf{k} = \cos\theta\cos\phi\,\mathbf{e}_x + \sin\theta\,\mathbf{e}_y + \cos\theta\sin\phi\,\mathbf{e}_z, \tag{2.21a}$$

$$\mathbf{u}(\mathbf{r}_2) = -\frac{\sigma}{2}\left|\frac{du}{dy}\right| \sin\theta\,\mathbf{e}_x, \quad \text{and} \quad d\mathbf{k} = \cos\theta\, d\theta\, d\phi. \tag{2.21b, c}$$

Thus by making use of equations (2.13), (2.16) and (2.21) and integrating with respect to $\mathbf{q}\,.\,\mathbf{k}$, we may write (2.20) as

$$\begin{aligned}\mathbf{T} = -\tfrac{1}{4} m\sigma^3 n^2 \overline{v^2} g_0(\sigma; \nu) \int_{\phi=0}^{2\pi} \int_{\theta=-\frac{1}{2}\pi}^{\frac{1}{2}\pi} \mathbf{kk}\, \mathrm{erfc}\,(-2^{-\frac{1}{2}} R\cos\phi\sin\theta\cos\theta) \\ \times \Big[(2/\pi)^{\frac{1}{2}} R\cos\phi\sin\theta\cos\theta \exp(-\tfrac{1}{2}R^2\cos^2\phi\sin^2\theta\cos^2\theta) \\ + (1 + R^2\cos^2\phi\sin^2\theta\cos^2\theta)\,\mathrm{erfc}\left(-\frac{R}{\sqrt{2}}\cos\phi\sin\theta\cos\theta\right)\Big] \cos\theta\, d\theta\, d\phi.\end{aligned} \tag{2.22}$$

3. Solutions for the components of the stress tensor

Although we have mentioned the precollision velocity fluctuation $\overline{v^2}^{\frac{1}{2}}$ and the mean shear to fluctuation velocity ratio $R = \sigma|du/dy|/\overline{v^2}^{\frac{1}{2}}$, little has been said about how their magnitudes are established. Physically, we can describe the process as follows. Consider a mass of granular material composed of rough, inelastic particles contained between two horizontal, rough, parallel, stationary plates. Suppose that the upper plate is set into motion parallel to its own plane so as to generate a constant shear rate du/dy within the granular material. The velocity fluctuations will increase in magnitude until the energy dissipation in the interior of the granular mass is equal to the mechanical work expended in moving the upper plate. Part of the 'quasi-thermal' energy associated with the particle fluctuations is turned into thermal energy during the inelastic collisions and frictional rubbing between particles. The heat so generated will be carried away by convection of the interstitial fluid and by conduction. In this way the final equilibrium, steady-state flow will be reached. Thus R will take on different values depending upon the properties of the solid particles such as their coefficient of restitution and the surface frictional properties. For a granular flow of nearly elastic solid particles with an interstitial fluid of negligible density, it seems reasonable to expect R to be about 1.

The preceding analysis to derive the stress tensor (2.22) has assumed smooth, perfectly elastic granules. The model contains no mechanism to permit dissipation and thus there is no way of using the present analysis directly to calculate R. To proceed, we shall simply regard R as a parameter and compute the components of the stress tensor over the complete range $0 < R < \infty$. The resulting stresses will then be compared with experiments for ranges of R that seem appropriate for each situation.

In general, the evaluation of (2.22) for $\mathbf{T}$ requires numerical integration. However, for small and large values of R, one may obtain simple asymptotic solutions which have straightforward physical interpretations.

3.1. *Solution for small R*

In addition to providing the asymptotic behaviour for the numerical solutions to be discussed later in this section, the small R solution has a specific physical interpretation. The limit $R \to 0$ is equivalent to the case in which the mean shear characteristic velocity $\sigma|du/dy|$ tends to zero with the fluctuation velocity $(\overline{v^2})^{\frac{1}{2}}$ fixed, and this must correspond to a situation in which the two velocities are *not* directly related. A fluidized bed subjected to a small shear is an obvious example. Carlos & Richardson (1968) measured the velocity fluctuations in fluidized beds having essentially no mean motion and found the magnitude of $\overline{v^2}$ to be a function of the fluidizing velocity. Thus the small R solution may be applied to the prediction of the effective viscosity of fluidized beds.

Expanding the integrand of (2.22) for small R and integrating term-by-term yields

$$\mathbf{T} = -2\nu g_0(\sigma;\nu)\rho_s\overline{v^2}\begin{pmatrix}1&0&0\\0&1&0\\0&0&1\end{pmatrix} + \frac{6}{5}\left(\frac{2}{\pi}\right)^{\frac{1}{2}}\nu g_0(\sigma;\nu)\rho_s\sigma\frac{du}{dy}\overline{v^2}^{\frac{1}{2}}\begin{pmatrix}0&1&0\\1&0&0\\0&0&0\end{pmatrix} + O(R^2), \tag{3.1}$$

where $\rho_s = nm$ is the mass density of the solid particles and the solids fraction

$$\nu = \tfrac{1}{6}\pi n\sigma^3.$$

The first term is an isotropic pressure arising from the velocity fluctuations associated with the interparticle collisions; there is no dependence upon shear rate. The second term, which depends linearly upon the shear rate, contains only two stress components, $T_{xy} = T_{yx}$. 'Non-Newtonian' effects appear in the third, $O(R^2)$ term where the stresses depend upon the square of the shear rate.

From this analysis the effective viscosity for a fluidized bed, *at low shear rates*, is

$$\mu_{\text{eff}} = \frac{6}{5}\left(\frac{2}{\pi}\right)^{\frac{1}{2}} \nu g_0(\sigma;\nu)\rho_s\sigma\,\overline{v^2}^{\frac{1}{2}}. \tag{3.2}$$

However, we shall leave a detailed discussion of this prediction to a later paper.

3.2. *Large R solution*

We now consider the solution as $R \to \infty$, with the precollision perturbation velocity $\overline{v^2}^{\frac{1}{2}}$ vanishing while the shear rate du/dy is fixed. We examine this limit not merely for a verification of the numerical integrations (§ 3.3), but also because it may have relevance to granular systems which possess considerable internal damping. Such damping might arise in the case of a shear flow in which the interstitial fluid is a dense viscous liquid. Immediately after each collision the particles involved may have velocities different from the mean velocity but because of the high density and viscosity of the interstitial fluid the particle velocities quickly regress towards the mean value prior to the next collision. Thus the precollision perturbation velocity $\overline{v^2}^{\frac{1}{2}}$ tends toward zero and R is very large. It should be noted that *in this limit* $\overline{v^2}^{\frac{1}{2}}$ is *not* related or analogous to the Reynolds' stresses or the intensity of a turbulent flow of a continuum. The Reynolds' stresses are obtained from a temporal average whereas $\overline{v^2}^{\frac{1}{2}}$ for the granular flow is defined by an ensemble average of grain velocities *just prior to collision*. When the turbulent fluctuation-velocities in a continuum are zero, then the Reynolds' stresses and the turbulent momentum transfer is zero. However, because of the finite particle size in a granular shear flow, collisions can occur and momentum can still be transferred even when the precollisional perturbation velocity $\overline{v^2}^{\frac{1}{2}}$ is zero.

For $R \to \infty$, the complementary error functions in the integrand of (2.22) obey

$$\operatorname{erfc}[-2^{-\frac{1}{2}}R\cos\phi\sin\theta\cos\theta] \to \begin{cases} 2 & \text{for} \quad (\cos\phi\sin\theta\cos\theta) > 0 \\ 0 & \text{for} \quad (\cos\phi\sin\theta\cos\theta) < 0 \end{cases} \tag{3.3}$$

and hence the integrations in (2.20) need only be carried out over the upstream faces of the collision sphere, i.e. over $0 \leqslant \theta \leqslant \frac{1}{2}\pi$ for $-\frac{1}{2}\pi \leqslant \phi \leqslant \frac{1}{2}\pi$ and over $-\frac{1}{2}\pi \leqslant \theta \leqslant 0$ for $\frac{1}{2}\pi \leqslant \phi \leqslant \frac{3}{2}\pi$. For large R, (2.20) may be integrated by the method of steepest descent to yield

$$\mathbf{T} = -\frac{6}{\pi}\nu g_0(\sigma;\nu)\rho_s\left(\sigma\frac{du}{dy}\right)^2 \int \mathbf{kk}(\cos\phi\sin\theta\cos\theta)^2\cos\theta\,d\theta\,d\phi. \tag{3.4}$$

Further integration for each stress component over the upstream faces of the collision sphere yields

$$\mathbf{T} = -\frac{12}{35}\nu g_0(\sigma;\nu)\rho_s\left(\sigma\frac{du}{dy}\right)^2 \begin{pmatrix} 1 & \frac{8}{3\pi} & 0 \\ \frac{8}{3\pi} & 1 & 0 \\ 0 & 0 & \frac{1}{3} \end{pmatrix} + O\left(\frac{1}{R^3}\right). \tag{3.5}$$

Reversing the direction of the shear flow and repeating the calculation will leave the normal stresses unchanged, but will reverse the sign of the shear stresses. The stress tensor should therefore be written as

$$\mathbf{T} = -\tfrac{12}{35}\nu g_0(\sigma;\nu)\rho_s\left(\sigma\frac{du}{dy}\right)^2\begin{pmatrix}1&0&0\\0&1&0\\0&0&\frac{1}{3}\end{pmatrix} + \frac{32}{35\pi}\nu g_0(\sigma;\nu)\rho_s\sigma^2\frac{du}{dy}\left|\frac{du}{dy}\right|\begin{pmatrix}0&1&0\\1&0&0\\0&0&0\end{pmatrix} + O\left(\frac{1}{R^3}\right). \tag{3.6}$$

To first order, we obtain both shear and normal stresses proportional to the square of both particle diameter and shear rate. The normal stresses are unequal:

$$T_{xx} = T_{yy} = 3T_{zz}.$$

The ratio of shear to normal stress, $|T_{xy}/T_{yy}| = 8/3\pi = \tan 40{\cdot}3°$.

It is interesting to compare these results with Bagnold's (1954) measurements of shear and normal stresses developed when neutrally buoyant wax spheres suspended in water were sheared in a coaxial-cylinder Couette flow apparatus. Since the analysis has neglected the interstitial fluid, and thus the explicit effects of the fluid on the collision dynamics as well as the fluid contributions to the momentum flux, we should not necessarily expect a close correspondence between the theory and the experiments. The neglect of the momentum flux due to the fluid will underestimate the stresses but the absence of the interstitial fluid will cause the solid-to-solid collisional momentum transfer to be overestimated. The two errors tend to cancel each other and thus the theory as $R \to \infty$ *may* be more accurate than one might initially expect. With these thoughts in mind, we have made a tentative comparison in figure 6 of the stresses obtained from (3.6) with those measured by Bagnold (1954). We have treated Bagnold's data by first non-dimensionalizing his stresses by dividing them by $\rho_s(\sigma\, du/dy)^2$, then plotting the non-dimensional stresses *for a given solids fraction* ν against $(du/dy)^{-1}$, and finally extrapolating the curve through these results to intersect the stress axis at $(du/dy)^{-1} = 0$. The data points attributed to Bagnold on figure 6 correspond to the intercept values. Note that, if we had plotted Bagnold's raw data, the agreement between his experiments and (3.6), in fact, would be slightly closer. By treating his data as described, we should obtain values conforming to the *grain-inertia* region, and presumably more appropriate for comparison with the theory.

Although the predicted shear stress T_{xy} is too high and the predicted normal stress T_{yy} is too low (figure 6), both stresses are of the right order of magnitude and their variations with concentration ν are correct, at least up to concentrations of about 0·5. For $\nu \lesssim 0{\cdot}5$ the experimental stresses increase much more rapidly with ν than do those predicted by (3.6). Recall that, to calculate the stresses, we have used (2.4) which underestimates $g_0(\sigma;\nu)$ for $\nu \lesssim 0{\cdot}5$.

There is also the possibility that, in the experiments at the higher concentrations, groups of particles locked together and that the actual shear took place over a gap *narrower* than the annular gap between the cylindrical walls of the apparatus. A crude way to estimate the result of such lockings is first to imagine that the total gap h is divided into two regions of constant concentration (figure 7), a locked region where the solids fraction is ν_L and a shear region of width δ where solids fraction is the

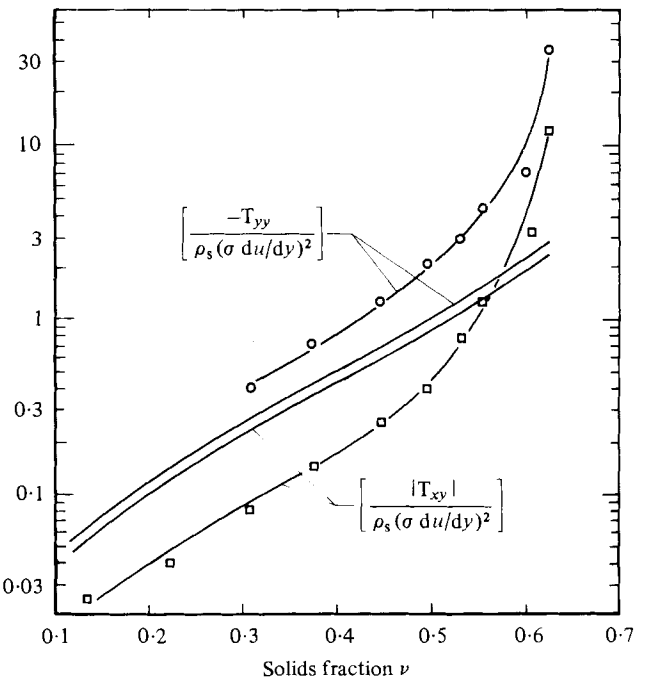

FIGURE 6. Comparison of stresses predicted for $R \gg 1$ with experimental measurements of Bagnold (1954). ——, present theory for $R \gg 1$ (equation (3.6)); ○ and □, Bagnold's data for normal and shear stresses respectively.

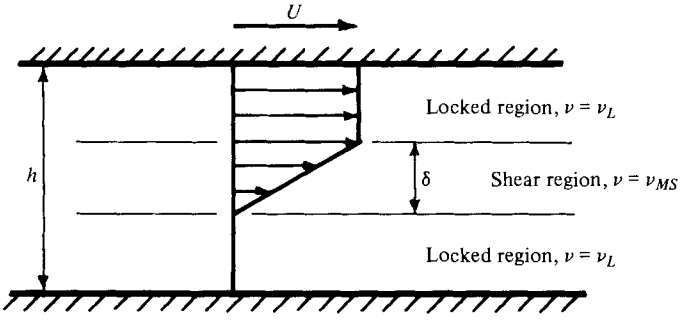

FIGURE 7. Formation of locked and shearing regions in viscometric apparatus.

maximum value ν_{MS} at which continued shear can occur. Take one wall of the shear apparatus to be stationary and the other moving with velocity U. The mean concentration $\bar{\nu}$ (which is all that Bagnold could measure in his experiment) can be expressed as

$$\bar{\nu} = \nu_{MS}(\delta/h) + \nu_L(1-\delta/h). \tag{3.7}$$

We can then express the real shear rate $(du/dy)_R = U/\delta$ in terms of the apparent shear rate $(du/dy)_A = U/h$ by using (3.7):

$$\left(\frac{du}{dy}\right)_R = \frac{h}{\delta}\left(\frac{du}{dy}\right)_A = \left(\frac{\nu_L - \nu_{MS}}{\nu_L - \bar{\nu}}\right)\left(\frac{du}{dy}\right)_A. \tag{3.8}$$

Thus for mean solids fractions $\bar{\nu}$ greater than ν_{MS}, the stress tensor for a given apparent shear rate may be determined from equation (3.6) applied at $\nu = \nu_{MS}$ and

$$du/dy = (du/dy)_R,$$

i.e.

$$\mathbf{T}\left(\bar{\nu}, \left(\frac{du}{dy}\right)_A\right) = \mathbf{T}\left(\nu = \nu_{MS}, \frac{du}{dy} = \left(\frac{du}{dy}\right)_R\right) \quad \text{for} \quad \bar{\nu} \geqslant \nu_{MS}. \tag{3.9}$$

We take ν_L to be about 0·64, corresponding to a random dense packing, and ν_{MS} to be 0·5, which is a little less than the value of 0·52 for a simple cubic packing of spheres (this comparison gives a physical feeling for the magnitude of ν_{MS} but it is not meant to imply that the spheres are actually moving in a regular array). Then (3.9) predicts rates of increase of the stresses which are close to Bagnold's measurements.

Finally, it should be emphasized that the locking model is a crude and tentative one. At moderate concentrations, the particle locking may occur, not in the definite bands as shown in figure 7, but in clusters or groups of particles which may form and break up intermittently over the full gap between the viscometer walls.

3.3. *General solution for arbitrary R*

For the general case of arbitrary values of R, integration of (2.22) must be performed numerically. This was done using the standard subroutine D01DAF from the NAG Fortran Library. A little care had to be exercised in its use because the integrand contained narrow peaks, often on the boundaries of the range of integrations; nevertheless, results correct to three significant figures were easily obtained.

The results of numerical integrations together with the asymptotes for small and large R are shown in figure 8 in the form of nondimensional stress components

$$\tilde{T}_{ij} = |T_{ij}|/[\rho_s \nu g_0(\sigma;\nu)(\sigma\, du/dy)^2]$$

versus R. The normal stress $\tilde{T}_{xx}$ equals $\tilde{T}_{yy}$, not only in the two asymptotic solutions, but over the full range of R. From the previous asymptotic analyses it was found that all the non-dimensional stress components $\tilde{T}_{ij}$ approach constant values for large R. For small R, the non-dimensional normal stresses vary as R^{-2} and the shear stress $\tilde{T}_{xy}$ as R^{-1}. Note that the ratio of shear to normal stress $|T_{xy}/T_{yy}| \to 8/3\pi$ as $R \to \infty$, decreases with decreasing R, and approaches zero as $R \to 0$.

Savage & Sayed (1980) have performed experiments with dry granular materials where the interstitial fluid was air. Both shear and normal stresses were determined when various mean concentrations of granular material were sheared in an annular shear cell. These experiments are probably the most appropriate for comparison with the present analysis; results from them are shown in figure 9. In the experiments, it was assumed that the total stresses were the sum of two parts, (i) a *dry friction part* which was independent of the shear rate for a given concentration, plus (ii) a *dynamic part* which depended upon the square of the shear rate. Using least-square fits to the data points for a given concentration, it was possible to separate the total stress into these two parts. The data points shown in figure 9 correspond to the values of the dynamic part which were generally close to the total stresses. Results are shown for 1·0 mm diameter polystyrene spheres having a specific gravity of 1·095 and for 1·8 mm diameter Ballotini spherical glass beads having a specific gravity of 2·97. The

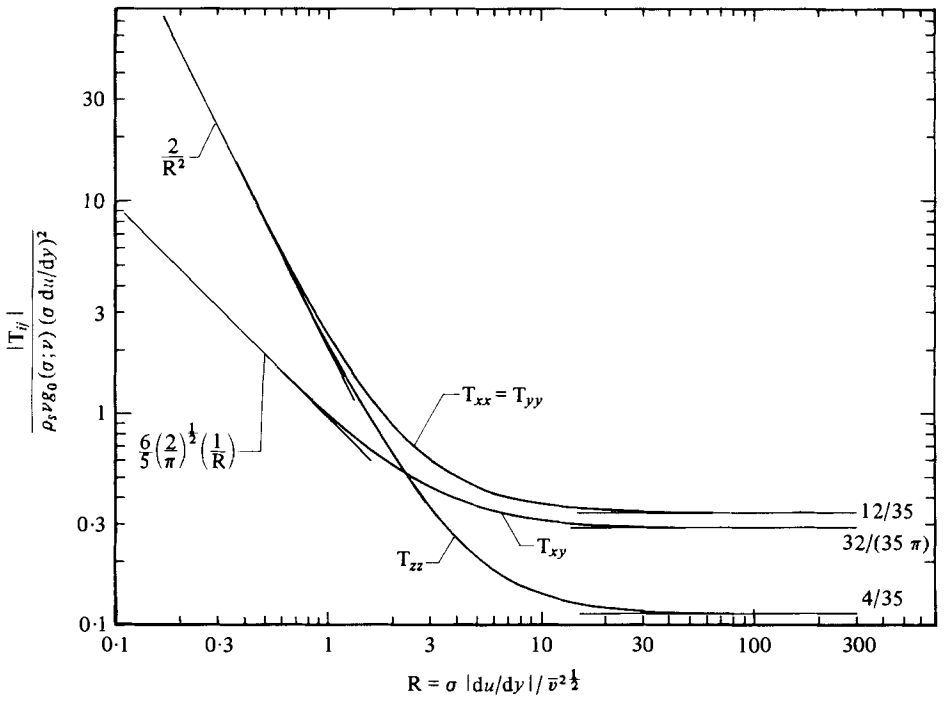

FIGURE 8. Variation of stress components with ratio of characteristic mean shear velocity to fluctuation velocity R.

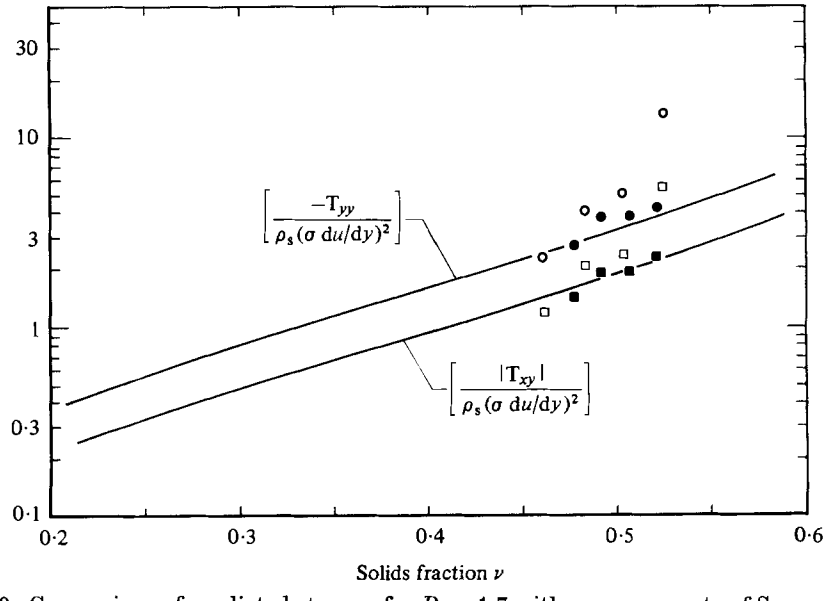

FIGURE 9. Comparison of predicted stresses for $R = 1{\cdot}7$ with measurements of Savage & Sayed (1980) for dry granular materials. ——, present theory for $R = 1{\cdot}7$; ○ and □, data of Savage & Sayed for normal and shear stresses respectively, open symbols are for 1·0 mm polystyrene spheres and solid symbols are for 1·8 mm Ballotini glass beads.

non-dimensional stresses for the two materials are similar up to a concentration of about 0·48, where the polystyrene beads begin to show a much more rapid increase of stress with concentration. The rapid increase is very likely to be associated with particle locking as described in § 3.2, but it is not obvious why locking should occur at lower concentrations in the tests with polystyrene beads. The phenomenon *may* be related to differences in particle size distributions for the two materials used in the tests.

The theoretical curves shown on figure 9 correspond to values of $R = 1{\cdot}7$. As mentioned previously, the present theoretical model cannot, as it stands, be used to determine the value of R; one is only guided by the intuitive feeling that R should be of order one for smooth, hard elastic particles like glass beads. Our choice of the value of the parameter $R = 1{\cdot}7$ has been made to yield theoretical stresses consistent with the experimental values. Nevertheless, it is seen that the predicted ratios of shear stress to normal stress $|T_{xy}/T_{yy}|$ are close to the experimental values and the glass beads, at least, show the proper variations of stresses with ν over the small range of ν covered in the tests.

4. Concluding remarks

A theory for the stresses developed during rapid shear of granular materials has been presented. The analysis was developed in terms of the parameter R, which is the ratio of the characteristic mean shear velocity to the particle fluctuation velocity. The analysis was applied to study three different physical situations, corresponding to different values of the parameter R; namely, (i) fluidized beads ($R \ll 1$), (ii) dry granular flows ($R = O(1)$), and (iii) Bagnold's granulo-viscous flow ($R \gg 1$). Since the analysis has neglected any effect of the interstitial fluid, the application of the analysis to this third situation is tentative and likely, to some degree, to be inappropriate. The level of agreement between the theory and experimental observations is encouraging and suggests that further refinements of the present simple theory would be worth developing.

The weak link in the present analysis is the inability to determine R. If we consider rough, inelastic particles having finite rotary inertia, it may be possible to determine R explicitly by establishing a balance between the input mechanical work and the energy dissipation in the sheared granular mass. This type of analysis could also determine the contribution to the total stress arising from rate-independent, Coulomb-type, dry frictional rubbing as well as the dynamic contribution described in the present paper.

The present analysis has assumed that the particle velocity fluctuations are isotropic and that there is no correlation between individual particle velocities. The collisional pair distribution function has been determined by a simple kinematic argument. Refinement here may require a rather strong departure from the simple procedure followed in the present paper.

It should be of interest to include, in a simple way, the momentum flux due to the interstitial fluid so that the analysis could be applied to cases in which the fluid and particle densities are of the same order. For the case of high concentrations a more sophisticated model for locking could be undertaken.

Grateful acknowledgement is made to the Natural Sciences and Engineering Research Council of Canada for support of this work. S.B.S. is indebted to Professor G. K. Batchelor for his hospitality at the Department of Applied Mathematics and Theoretical Physics, University of Cambridge, where this paper was written.

REFERENCES

ALDER, B. J. & HOOVER, W. G. 1968 Numerical statistical mechanics. In *Physics of Simple Liquids* (ed. H. N. V. Temperley, J. S. Rowlinson & G. S. Rushbrooke). North Holland.

BAGNOLD, R. A. 1954 Experiments on a gravity-free dispersion of large solid spheres in a Newtonian fluid under shear. *Proc. Roy. Soc.* A **225**, 49–63.

BATCHELOR, G. K. 1976 Developments in microhydrodynamics. In *Theoretical and Applied Mechanics* (ed. W. T. Koiter). Proc. IUTAM Congress, Delft, North Holland.

BAXTER, R. J. 1968 Percus–Yevick equation for hard spheres with surface adhesion. *J. Chem. Phys.* **49**, 2770–2774.

BAXTER, R. J. 1971 Distribution functions. *Physical Chemistry, An Advanced Treatise.* Vol. VIIIA. *Liquid State* (ed. D. Henderson). Academic.

BORN, M. & GREEN, H. S. 1947 A general kinetic theory of liquids. III. Dynamical properties. *Proc. Roy. Soc.* A **190**, 455–474.

CARLOS, C. R. & RICHARDSON, J. F. 1968 Solids movement in liquid fluidized beds. I. Particle velocity distribution. *Chem. Engng Sci.* **23**, 813–824.

CARNAHAN, N. F. & STARLING, K. E. 1969 Equations of state for non-attracting rigid spheres. *J. Chem. Phys.* **51**, 635–636.

CHAPMAN, S. & COWLING, T. G. 1970 *The Mathematical Theory of Non-Uniform Gases*, 3rd edn. Cambridge University Press.

CHENG, D. C.-H. & RICHMOND, R. A. 1978 Some observations on the rheological behaviour of dense suspensions. *Rheol. Acta* **17**, 446–453.

CROXTON, C. A. 1974 *Liquid State Physics.* Cambridge University Press.

FABER, T. E. 1972 *An Introduction to the Theory of Liquid Metals.* Cambridge University Press.

GADALA-MARIA, F. 1979 The rheology of concentrated suspensions. Ph.D. dissertation, Stanford University.

GOLDSMITH, H. L. & MASON, S. G. 1967 Microrheology of dispersions. *Rheology: Theory and Applications*, vol. 4 (ed. F. R. Eirich). Academic.

GREEN, H. S. 1969 *The Molecular Theory of Fluids.* Dover.

HANSEN, J. P. & MCDONALD, I. R. 1976 *Theory of Simple Liquids.* Academic.

HENDERSON, D. 1971 *Physical Chemistry, An Advanced Treatise*, vol. 8A, *Liquid State.* Academic.

JEFFREY, D. J. & ACRIVOS, A. 1976 The rheological properties of suspensions of rigid particles. *Am. Inst. Chem. Engng J.* **22**, 417–432.

JENKINS, J. T. & COWIN, S. C. 1979 Theories for flowing granular materials. *Mechanics Applied to the Transport of Bulk Materials.* A.S.M.E. AMD-**31** (ed. S. C. Cowin).

KANATANI, K. 1979 A micropolar continuum theory for the flow of granular materials. *Int. J. Engng Sci.* **17**, 419–432.

KIRKWOOD, J. G., BUFF, F. P. & GREEN, M. S. 1949 The statistical mechanical theory of transport processes. III. The coefficients of shear and bulk viscosity of liquids. *J. Chem. Phys.* **17**, 988–994.

LEBOWITZ, J. L. 1964 Exact solution of generalized Percus–Yevick equation for a mixture of hard spheres. *Phys. Rev.* A **133**, 895–899.

MANSOORI, G. A., CARNAHAN, N. F., STARLING, K. E. & LELAND, T. W. 1971 Equilibrium thermodynamic properties of the mixture of hard spheres. *J. Chem. Phys.* **54**, 1523–1525.

MARBLE, F. E. 1964 Mechanism of particle collision in the one-dimens.ional dynamics of gas–particle mixtures. *Phys. Fluids* **7**, 1270–1282

McTIGUE, D. F. 1978 A model for stresses in shear flow of granular material. *Proc. U.S.–Japan Seminar on Continuum Mechanical and Statistical Approaches in the Mechanics of Granular Materials*, pp. 266–271. Tokyo: Gakujutsu Bunken Fukyu-kai.

McTIGUE, D. F. 1979 A nonlinear continuum model for flowing granular materials. Ph.D. dissertation, Stanford University.

REE, F. H. 1971 Computer calculations for model systems. *Physical Chemistry, An Advanced Treatise*, vol. 8A, *Liquid State* (ed. D. Henderson). Academic.

REED, T. H. & GUBBINS, K. E. 1973 *Applied Statistical Mechanics*. McGraw-Hill.

SAVAGE, S. B. 1979 Gravity flow of cohesionless granular materials in chutes and channels. *J. Fluid Mech.* **92**, 53–96.

SAVAGE, S. B. & SAYED, M. 1980 Experiments on dry cohensionless materials in an annular shear cell at high strain rates. Presented at *EUROMECH* 133 – *Statics and Dynamics of Granular Materials. Oxford University.*

SCHOFIELD, A. N. & WROTH, C. P. 1968 *Critical State Soil Mechanics*. McGraw-Hill.

SOO, S. L. 1967 *Fluid Dynamics of Multiphase Systems*. Blaisdell.

TEMPERLEY, H. N. V., ROWLINSON, J. S. & RUSHBROOKE, G. S. 1968 *Physics of Simple Liquids*. North Holland.

THIELE, E. J. 1963 Equation of state for hard spheres. *J. Chem. Phys.* **39**, 474–479.

WERTHEIM, M. S. 1963 Exact solution of the Percus–Yevick integral equation for hard spheres. *Phys. Rev. Lett.* **10**, 321–323.

WOOD, W. W. 1968 Monte Carlo studies of simple liquid models. *Physics of Simple Liquids* (ed. H. N. V. Temperley, J. S. Rowlinson & G. S. Rushbrooke). North Holland.

ZIMAN, J. M. 1979 *Models of Disorder*. Cambridge University Press.